RSC Advances

ROYAL SOCIETY OF CHEMISTRY

www.rsc.org/advances

RSC Advances

RSCPublishing

PAPER

Fabrication of Porous TiO_2-SiO_2 Multifunctional Anti-reflection Coatings by Sol-Gel Spin Coating Method

Qiangqiang Mao,[a] Dawen Zeng,[a,b] Keng Xu,[a] and Changsheng Xie[b]

In this study, we reported here that an antireflective coating with multifunctional properties, including high transparency, self-cleaning and abrasion resistance， was prepared by a facile sol-gel spin-coating method. The average transmittance of single coated glass substrates was greater than 93% in the wavelength range of 300-1000 nm compared to 90.1% for bare glass substrate. The photocatalytic activity of the coatings showed a close dependence on content of TiO_2 nanoparticles. The coatings showed the ability to decompose air borne organic contaminants (gaseous benzene) and applied contaminants (fingerprints) under Uv irradiation when the content of TiO_2 was greater than 10%. After illuminated by Uv light, the TiO_2-SiO_2 coatings showed hydrophilic property with water contact angle about 1°, which favored greatly the self-cleaning function of the coatings. When the content of TiO_2 was 10%, the critical load of the coating increased up to 305 μN as compared with that of the base-catalyzed SiO_2 coating (198 μN), which indicated the abrasion resistance property of this coating. This approach suggested novel opportunities to a variety of practical applications, including windows of high rise buildings, solar thermal collectors and solar cells cover glasses, etc.

Introduction

Anti-reflection coatings (ARCs) have been widely used in energy-related applications including solar thermal collectors, windows of high rise buildings and covers of solar cells.[1-5] Up to now, many research works have been conducted to improve the transmittance property of the ARCs.[6-8] But, a coating with only anti-reflection capacity will not satisfied the increasing demands of more competitive technologies and practical applications.[9] More and more recent research works consolidate the interest and feasibility of elaboration of multifunctional coatings, such as anti-fogging, anti-abrasion and self-cleaning coatings.[7,10,11]

For outdoor and solar energy-related applications, anti-reflection and self-cleaning (AR-SC) are two practical properties, which have been achieved on glass substrate by SiO_2 and TiO_2 films, respectively.[7,9,10,12-14] On the one hand, porous SiO_2 was considered to achieved high anti-reflection property due to its tunable refractive index properties.[6,7,15,16] On the other hand, TiO_2 film showed self-cleaning property because of its two photo-induced phenomena: photocatalysis and photo-induced hydrophilicity.[17-20] TiO_2 could decompose the organic pollutant absorbed on the surface of film under Uv light irradiation. And dirt particles could be washed off from the surface when water droplet rolled over the surface of the film.[2,19,20]

In the past few years, two main methods have been used to fabricate AR-SC coatings on glass substrate.[7,9,10,12-14] In the first method, SiO_2 and TiO_2 particles were deposited on substrate by various techniques, such as dip-coating, spin-coating and spray pyrolysis techniques, to obtain double layer coating.[9,10,13,14] The bottom SiO_2 and the top TiO_2 films were prepared to provide anti-reflection and self-cleaning properties, respectively. As the thickness of TiO_2 layer increased, the transmittance of the coating decreased sharply with the self-cleaning capacity increased.[10] In the second method, the co-deposition of TiO_2 and SiO_2 particles to form a single layer ARCs.[7,12] However, the refractive index of TiO_2 was high ($n>1.45$), so the content of TiO_2 and the structure of the coating has to be controlled.[2] According to previous reports,[2,6,7] the index of the coating could be lowered by introducing porosity and reducing the particle size of TiO_2. Meanwhile, the more photo-active of TiO_2 nanoparticle was due to the organic molecules were decomposed at or near the TiO_2 surface and its wider band gap.[18] So a coatings with a high porosity and TiO_2 nanoparticle will maintain both the high transmittance and self-cleaning property for a long time, which was important when a coating was used in practical applications. But only a few research works has focused on the preparation of AR-SC coatings with

TiO_2 nanoparticles to maintain high antireflective and photocatalytic self-cleaning properties.[21]

Recently, there were mainly two approaches to investigate the self-cleaning property of these AR-SC coatings. Some authors investigated the self-clean capacity of coatings by measuring the degradation of organic films deposited on the surface of the coatings throughout water contact angle measurement [13,22] and IR-spectroscopy.[7,12] Degradation of some liquid pollutants, including rhodamin B[14] and methylene blue,[9,10] was also used to measure the self-cleaning property of the coatings. On the other hand, during practical application process, the surface of the anti-reflection coating was easily polluted by various pollutants in the air and the applied contaminants. Those pollutants would dramatically deteriorate the long term transmittance property of the anti-reflection coatings. However, few researchers measured the self-cleaning property of AR-SC coating by the degradation of gaseous pollutants and the applied contaminants.[7] But, during practical application process, those contaminants would dramatically deteriorate the long term transmittance property of the AR-SC coatings. Therefore, it is an interesting and important work to fabricate a coating with self-cleaning property to maintain the high anti-reflection property for a long time.

In this study, TiO_2-SiO_2 anti-reflection coating with multifunctional characteristics, including high transmittance, self-cleaning and abrasion resistance properties, was prepared by spin-coating method. The effect of content of TiO_2 nanoparticles on light transmittance, photocatalytic activity, hydrophilicity and abrasion resistance properties of the coatings was explored respectively. The combination of those properties provided promising outdoor uses, such as window of high rise buildings and solar thermal collectors.

Experimental

Materials

Tetraethyl orthosilicate (TEOS), ammonium hydroxide (NH_4OH), hydrochloric acid (HCl, 37%) and ethanol (EtOH) were purchased from Sinopharm Chemical Reagent. Titanium n-butoxide (n-Buti, 99%) was obtained from Alfa Aesar. All chemicals were used as received.

Preparation of Sol-Gel Spin Coatings

The base-catalyzed SiO_2 sol was prepared by mixing TEOS, EtOH, H_2O and NH_4OH with a molar ratio of 1:37:2:0.8. This solution was stirred for 4 h and aged at room temperature for 3 days. And then it was refluxed at 80 °C until the pH of the solution was about 6. TiO_2 sol was prepared by mixing n-Buti and EtOH, followed by the dropwise addition of an aqueous solution of HCl. The chemicals were mixed at a molar ratio n-Buti:EtOH:H_2O:HCl of 1:60:4:0.3. This sol was stirred for 4 h and aged at room temperature for 1 day. Both precursor solutions were mixed together to obtain sols with different TiO_2 concentrations.

The glass substrates (1 mm thick, 30*30 mm soda-lime glass) were cleaned with acetone, ethanol and distilled water by ultrasonic cleaning method, and then dried at 80 °C. The coatings were single deposited onto pre-cleaned glass slides by spin coating (8000 rpm, 20 s). The coated glass samples were dried in air at room temperature and were calcined at 500 °C for 30 min and cooled down to room temperature in the closed furnace.

Photocatalytic Activity

Photocatalytic performance of the coatings was evaluated by degrading gaseous benzene under irradiation of Uv light at ambient temperature in a 2 L cubic reactor, before which the air tightness of the reactor was tested. The Uv light was generated from a Xenon lamp (UV300, Aulight of China Co., LTD) with a wavelength range of 200 - 400 nm. After six pieces of the coated glass substrates (3*3 cm, each piece) were placed into the reactor, an amount of aqueous benzene was also injected within by a syringe. The bottom of the reactor was slightly heated (below 40 °C) to ensure benzene all evaporated. The analysis of the concentration of benzene and CO_2 was performed with a gas chromatography (GC9560, Shanghai Huaai Co., LTD). Each set of experiments was monitored for 3 h.

Characterization

The transmission spectra of the coated and uncoated glasses were measured by using Uv-vis transmittance spectra (Unico UV-2012PC) in the wavelength range of 200–1000 nm. The surface morphology of the coatings was characterized by scanning electron microscopy (SEM, Sirion 200). Transmission electron microscope (TEM) and high-resolution transmission electron microscope (HRTEM) characterizations were performed with a FEI Tecnai G220 microscope working at 200 kV. Chemical composition of the coating was defined by X-ray photoelectron spectroscopy (XPS, AXIS-ULTRA DLD-600W). The surface wettability of the coatings was studied by a contact angle/interface system (SL-200) with ±1° accuracy in atmospheric air at room temperature. Water droplets of 1μL were dropped carefully onto the coating surface. Nanoscratch test was carried out using the Tribolndenter system (Hysitron TI750) with a spherical diamond indenter tip.

Results and discussion

Anti-reflection Property

The effect of the content of TiO_2 on the transmittance of coatings was shown in Figure 1. According to the Uv-vis spectra, the coated glass substrates showed high anti-reflection. As shown in Figure 1a, in contrast to the transmittance of the base-catalyzed SiO_2 coating, the transmittance of the coatings decreased gradually in the range of 400-1000 nm with the content of TiO_2 increased from 2 to 20 wt%. The average transmittance of the coated glass substrate was decreased from 93.43% to 92.3% with the content of TiO_2 increased from 0% to 20% in the wavelength range 300-1000 nm compared to that (90%) of bare glass substrate, as shown in Figure 1b.

The refractive index of coating (n_c) was one parameter to its ideal anti-reflection property. According to the relevant research [23], the refractive index of porous coating can be calculated. The transmittance of the bare glass substrate is 90.6% at the wavelength

of 701 nm, and the refractive index was estimated to be 1.55. The transmittance of the different coatings (0%, 2%, 5%,10% and 20% TiO_2-SiO_2) at 701 nm were 94.6%, 94.2%, 94.0%, 93.5% and 93.1%, respectively. Then, the n_c were estimated to be 1.47, 1.48, 1.49, 1.50 and 1.51, respectively.

Therefore, according to the results of the experiments, the coatings could maintain the high transmittance when the content of TiO_2 was no more than 20%.

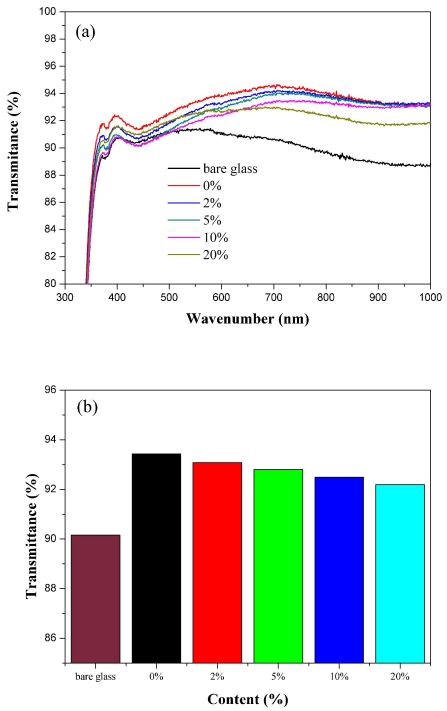

Figure 1. a) Transmittance spectra and b) average transmittance of the coatings with different contents of TiO_2.

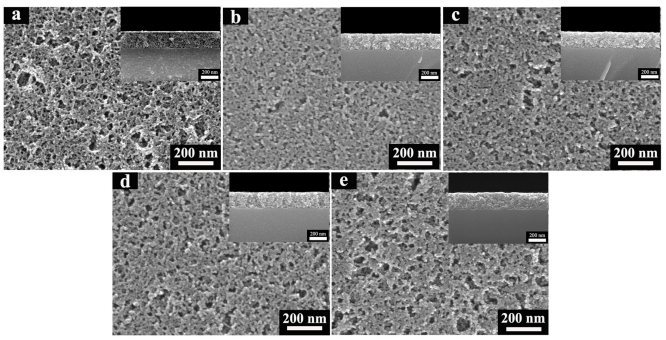

Figure 2. Scanning electron microscope micrographs for different coatings: a) base-catalyzed SiO_2 coating; b) 2% TiO_2-SiO_2 coating; c) 5% TiO_2-SiO_2 coating; d) 10% TiO_2-SiO_2 coating; e) 20% TiO_2-SiO_2 coating. The insets are the cross-sectional electron micrographs of each coating. The scale bars represent 200 nm.

Surface Morphology

FESEM images of the base-catalyzed SiO_2 and TiO_2-SiO_2 coatings were shown in Figure 2. As shown in Figure 2a-e, porous structures were generated on the surface of the coatings and the surface was changed with the increase in content of TiO_2. When the TiO_2 content was no more than 10% (Figure 2a-d), the size of most pores were less than 80 nm. The porosity of the coatings was helpful to trap and restrain the scattered and reflected light.[15] As a result; more light could transmit through the coating. Then, the coatings showed high transmittance property in the wavelength range (400-1000 nm). But, when the TiO_2 content was 20%, there were some large pores（about 100 nm）on the surface of the coating (Figure 2e). The pore size was about 10% of the incident light wavelength, which could lead to surface scattering.[16] This was maybe the main reason for the decrease of transmittance of this coating.

The thickness of TiO_2-SiO_2 coatings were also observed by cross section morphology of the coatings from FSEM images (Figure 2). The thickness of the coatings was about 200 nm. On the other hand, the thickness of the coating was corresponding to the maximum transmittance of those coatings[16]. As shown in Figure 1, the wavelength of the maximum transmittance of those coating has not changed significantly. This result also indicated the uniform thickness of those coatings.

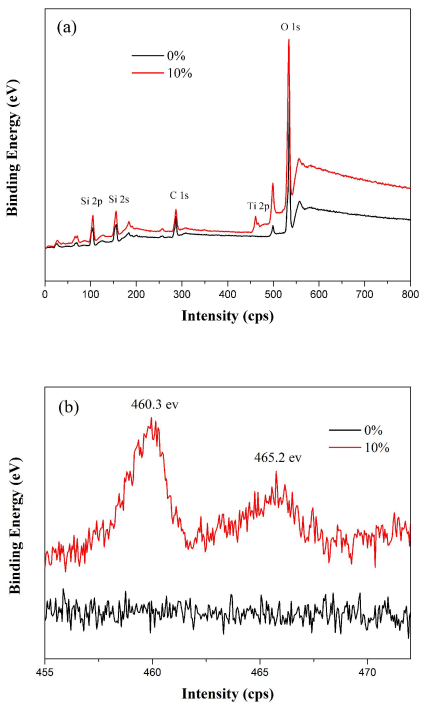

Figure 3. XPS spectra of 0% and 10%TiO_2-SiO_2 coating: a) survey spectra, b).Ti 2p.

Chemical Composition

XPS was used to determine the chemical composition of the surface of 10% TiO_2-SiO_2 coating, as shown in Figure 3. The appearance of the Ti 2p peak in the 10% TiO_2-SiO_2 coating confirmed the

introduction of TiO_2 (Figure 3b). The two peaks at 460.3 and 465.2 eV were the 2p 3/2 orbital and the 2p 1/2 orbital of the Ti atom,[24,25] respectively. The reported binding energy of Ti 2p3/2 for pure TiO_2 coating was 458.2 eV [24,25]. But, in this article, the Ti 2p 3/2 of the 10% TiO_2-SiO_2 coating was 460.3 eV. It showed a 1.1 eV of chemical shifts to the pure TiO_2 coating. In the similar research work, [24] the Ti 2p 3/2 binding energy of $(TiO_2)_{10}(SiO_2)_{90}$ coating shifted 1.25 eV as compared to that of pure TiO_2 coating. The chemical shifts of Ti 2p gave an evidence of the formation of interaction between SiO_2 and TiO_2 particles.

To get further indication of TiO_2 nanoparticles, the microstructures and crystalline of 10% TiO_2-SiO_2 powder were studied. TEM and HRTEM micrographs were shown in Figure 4. It was obvious that the sample was consisting of good crystal TiO_2 nanoparticles, which were dispersed in amorphous SiO_2 particles, as shown in Figure 4a. The average particle sizes of TiO_2 estimated from HRTEM micrographs were about 5 nm (Figure 4b). The spacing d=0.232 nm of 10% TiO_2-SiO_2 powders corresponded to the (004) plane of anatase TiO_2 phase [26, 27]. The nano-crystalline TiO_2 particles in this coating provided high photocatalytic property (Figure 5 and Figure 6).[25] And this size of TiO_2 nanoparticles could be made optically clear enough for commercial window use.[18]

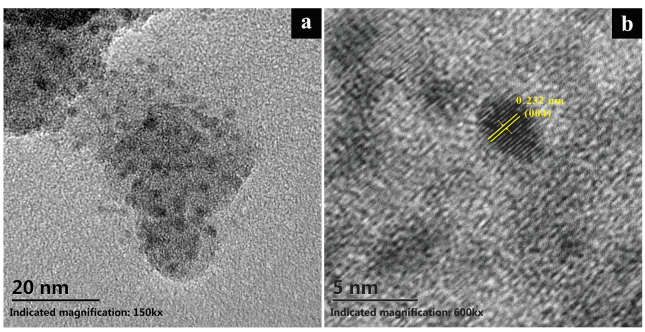

Figure 4. a) TEM micrograph of 10%TiO_2-SiO_2 powders and b) HRTEM micrograph of TiO_2 nanoparticles.

Table 1. The conversion of C_6H_6 and the amount of produced CO_2 of different coatings under Uv light irradiation.

	glass	0%	2%	5%	10%	20%
$\triangle C_6H_{6\,/ppm}$	32	60	61	64	68	76
$\triangle CO_{2\,/ppm}$	16	15	19	30	63	121
$\triangle CO_2/\triangle C_6H_6$	0.5	0.25	0.31	0.46	0.93	1.59

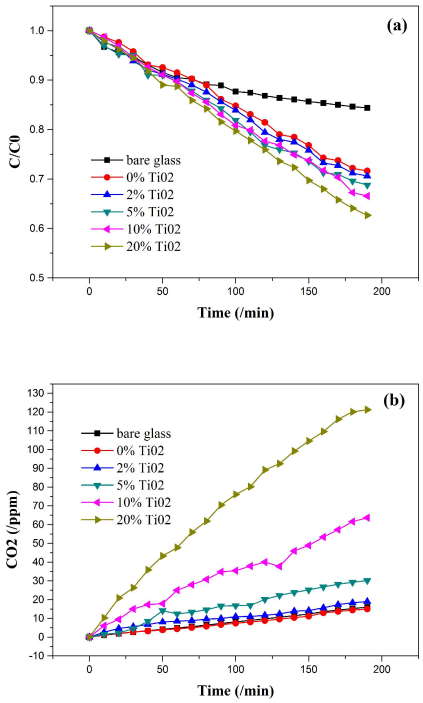

Figure 5. The curves of a) conversion of C_6H_6 and b) the amount of produced CO_2 of different coatings under Uv light irradiation.

Self-cleaning Properties

In this study, we investigated the self-cleaning property of coating by the degradation of air borne organic contaminants (gaseous benzene) and applied contaminants (fingerprints) under Uv irradiation.

On the one hand, photocatalytic activities of different coatings for degradation of gaseous benzene under Uv irradiation at ambient temperature were investigated. The conversion of benzene and the production of CO_2 were not observed when these samples were in dark. Figure 5 showed the photocatalytic activities of coatings with different concentrations of TiO_2 nanoparticles under Uv light irradiation. As shown in Figure 5a, the amount of benzene still decreased when there was only glass substrate and SiO_2 coating in the reactor. This was due to the adsorption of gaseous benzene. But the amount of adsorption is limit. On the other hand, the coatings in this article were porous coating, which can be seen in the SEM images (Figure 2). Thus, as shown in Figure 5a, all porous coatings have the good absorption effect of gaseous benzene. But the conversion amount of benzene was different. Then the conversion of benzene was not enough to evaluate the photocatalytic activity of the coatings. So the curves of the production of CO_2 of different coatings were also shown (Figure 5b). The production of CO_2 of bare glass and SiO_2 coating were merely about 15 ppm which was almost same as that of the blank test (no glass substrate, only with benzene and Uv-light irradiation), as shown in supporting information (Figure 10). This increasing may be due to the

increasing temperature of the reactor which was caused by the Uv-light irradiation during the test (about from 25 ℃ to 36 ℃). And the concentration of CO_2 was affected by the temperature of the gas when it was measured with a gas chromatography. This result also proved that the decrease of benzene of bare glass and SiO_2 coating was due to the absorption effect. As shown in Table 1, the production of CO_2 increased remarkably from 19 ppm to 121 ppm (Figure 5b and Table 1) and the contrast of generated carbon dioxide to the amount of degradation of benzene increased from 0.31 to 1.59, when the content of TiO_2 nanoparticles increased from 2% to 20%. Those results shown the amount of production of CO_2 was correlated to the total amount of TiO_2. The photocatalytic activity of the coatings was corresponding to the formation of anatase TiO_2 nanoparticles (Figure 4b).[26] From the above discussions, as the content of TiO_2 nanoparticles increased in the coatings, their photocatalytic activities gradually increased.

On the other hand, photocatalytic activities of 10% TiO_2-SiO_2 coating for decomposing of fingerprint under Uv irradiation at ambient temperature was investigated. During practical application, fingerprints will inevitably stick on the surface of coating. Then the anti-reflection property of the coating will be seriously affected. As shown in Figure 6, the fingerprint disappeared completely from the surface of the coating after irradiation with Uv light for 150 min. This result indicated that the self-cleaning property of this coating was useful to maintain high transmittance for a long time.

Surface Wettability

Water droplets could spread out to form a thin water film on a hydrophilic surface and then, dusts on the surface could be taken away easily, showing the self-cleaning ability.[2,19,20] Table 2 showed the contact angle of 1 μL water on the coatings with different content of TiO_2 (0%, 2%, 5%, 10%, 20% and 100%), respectively. The water contact angle of the SiO_2 coating was about 1°. The increase of the contact angle was proportional to the increase of the content of TiO_2 nanoparticles in the coatings. However, the wettability of the coatings became almost same after Uv irradiation. This was due to the special photo-induced hydrophilicity of TiO_2.[13,19,22] All coatings showed hydrophilic property with contact angle less than 1°, as shown in Table 2. On the other hand, we measured the duration of the photo-induced hydrophilicity of those TiO_2-SiO_2 coatings. The change of the contact angle in dark was shown in supporting information (Figure11). It seemed that the photo-induced hydrophilicity of those coatings was not permanent. The highly hydrophilic surface produced by Uv light irradiation gradually converted to less hydrophilic state in several days. But the hydrophilicity state can easily be recovered by exposing the coatings to Uv-light.

Adhesion Property

During practical application, the coated glass will be cleaned usually, thus the coating should have good abrasion resistance property. In this study, nanoscratch was performed to evaluate the abrasion resistance of the coating (10% TiO_2-SiO_2 coating), as shown in Figure 7-8. The critical load, Pc, is defined as the lateral load when the lateral load fluctuation occurs in the scratch test. It is a comprehensive index that it represents the carrying capacity of the coating/substrate.[28] It was mainly affected by the adhesive and hardness of the coating and substrate, the structure and thickness of the film. Figure 7 showed the load-distance curves of nanoscratch test of base-catalyzed SiO_2 coating and 10% TiO_2 - SiO_2 coating. The Pc of the base-catalyzed SiO_2 coating and 10% TiO_2-SiO_2 coating were 198 μN and 305 μN, respectively. This result pointed to excellent abrasion resistance property of this coating. It also could be identified in the AFM images of the scratches on the surface of two coatings (Figure 8). It was obviously that the 10% TiO_2-SiO_2 coating exhibited better scratch resistance property.

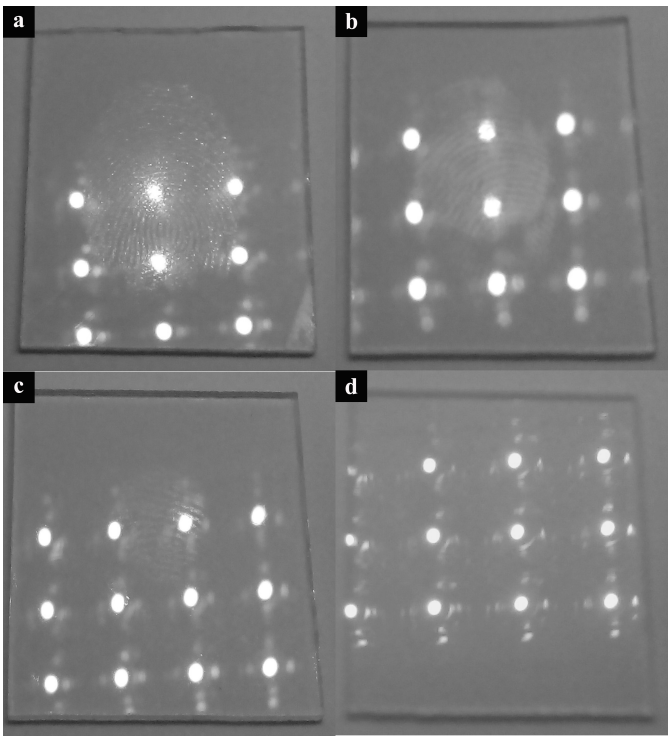

Figure 6. Photo-degradation of fingerprints applied on 10% TiO_2-SiO_2 coating surface upon exposure to simulated Uv light. a) after application of the fingerprint; b) after 60 min; c) after 120 min; d) after 150 min. The samples were briefly rinsed with water after 60 min to simulate the effect of water.

Table 2. Water contact angles (CA) of coatings with different content of TiO_2 (0%, 2%, 5%, 10%, 20% and 100%) before and after Uv irradiation for 90 min.

TiO2%	glass	0%	2%	5%	10%	20%	100%
CA (before)	38°	<1°	<1°	9°	15°	21°	51°
CA (after)	37°	<1°	<1°	<1°	<1°	<1°	<1°

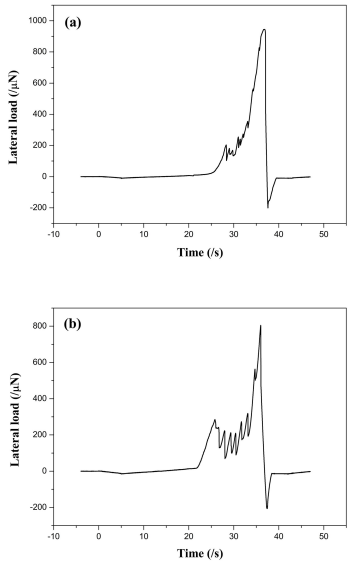

Figure 7. Loading-time curves of (a) the base-catalyzed SiO_2 coating and (b) the 10% TiO_2-SiO_2 coating.

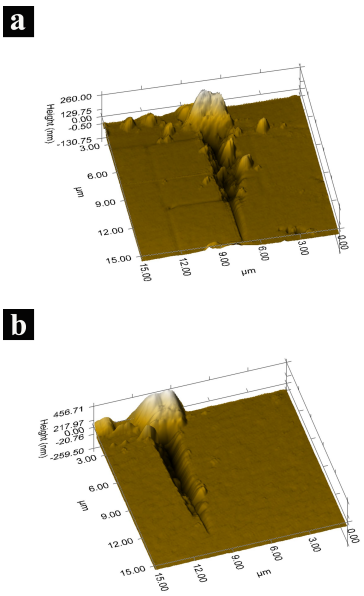

Figure 8. AFM images of scratch on the surface of (a) the base-catalyzed SiO_2 coating and (b) the 10% TiO_2-SiO_2 coating.

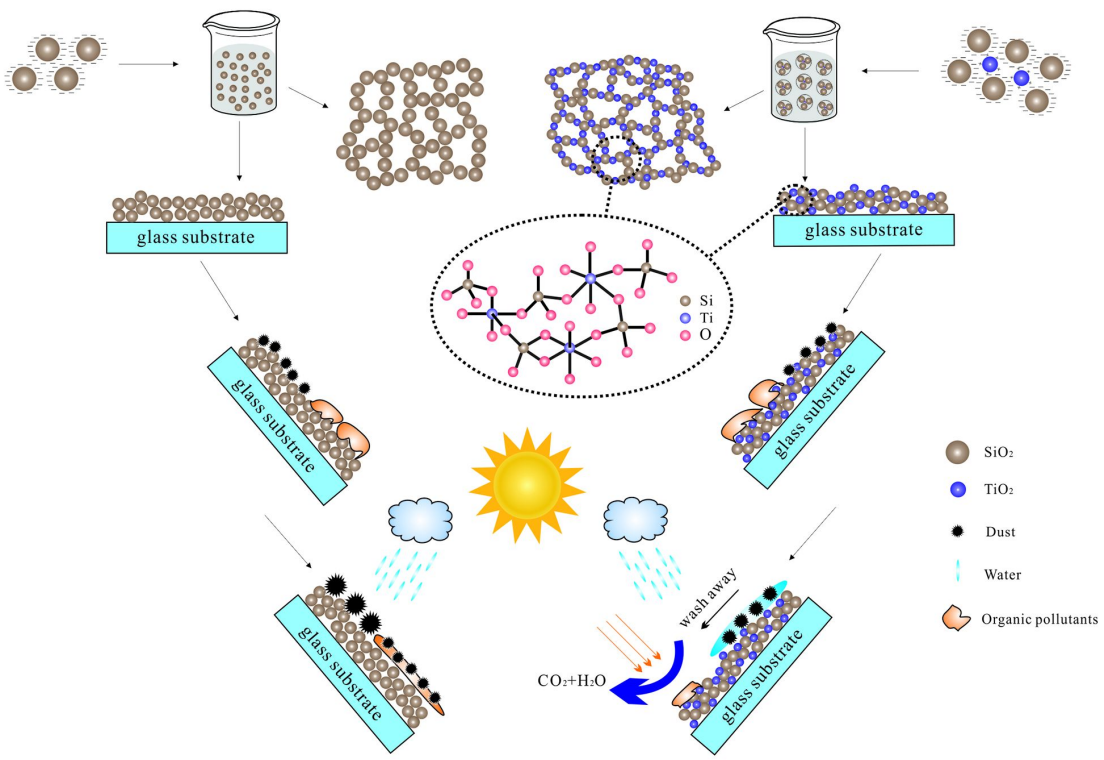

Figure 9. Schematic showing the preparation and the self-cleaning phenomena of the anti-reflection self-cleaning coating on glass substrate.

RSC Advances

RSCPublishing

PAPER

The preparation and the self-cleaning phenomena of the AR-SC coating were presented in Figure 9. The base-catalyzed SiO_2 particles were negatively charged and those particles repelled each other to form particulate sol.[8,16] In the base-catalyzed SiO_2 coating, individual SiO_2 particles kept intact only by point contact forces,[16] pointing to the poor mechanical robustness. On the other hand, the negatively charged SiO_2 particles in silica sol could selectively adsorb positive charged TiO_2 nanoparticles from the surrounding solution.[29] TiO_2 nanoparticles seemed to act as viscous glue between the silica particles. During the heat treatment process, ethanol solvent was evaporated and alkanol was burned; then pores with different sizes were appeared. In order to enhance the mechanical property, the neighboring particles were chemically bound to each other and to the surface through Ti-O-Si bonds (Figure 3b and Figure 9).[2] As shown in Figure 9, in particle application, organic pollutants and dirt particles will be stuck on the surface of coatings inevitably. The dirt particles will be easily aggregated in the organic pollutants, which may affect the anti-reflection effect of the coating. But, after Uv irradiation, the TiO_2 nanoparticles in the coating could exhibit the desired simultaneous property of photocatalysis and photo-induced hydrophilic. Then, the absorbed organic contaminants could be decomposed and the dust on the surface could be removed easily by the rainwater.

Conclusions

In this study, glass substrates were coated with TiO_2 and SiO_2 nanoparticles to achieve coating with both anti-reflection, self-cleaning and abrasion resistance properties by spin-coating method. The coated glass substrate exhibit high transmittance even the concentration of TiO_2 was up to 20%. The average transmittance of the coating (10% TiO_2-SiO_2) increased more than 2.3% as compared to uncoated glass substrate. Moreover, the photocatalytic activity of this coatings will lead to the decomposition of contaminants (gaseous benzene and fingerprints) keeping the surface clean and maintaining the high transmittance property. The photocatalytic and hydrophilic properties of coating provided the self-cleaning function. Further, this coating exhibited abrasion resistance property. The Pc of the coatings enhanced from 198 μN (0%) to 305 μN (10%), pointing to excellent abrasion resistance of this coating. The combined anti-reflection, self-cleaning and abrasion resistance properties should substantially improve the long-term optical properties of porous AR-SC coatings.

Acknowledgments

This work was supported by the National Basic Research Program of China (Project No. 2009CB939705 and 2009CB939702). Also, we thank the technology support by the Analytic Testing Center of HUST for carrying out FESEM and XPS analyses.

Note and references

[a] State Key Laboratory of Materials Processing and Die & Mould Technology, Huazhong University of Science and Technology (HUST), No. 1037, Luoyu Road, Wuhan 430074, PR China.
E-mail address: dwzeng@mail.hust.edu.cn.
[b] Nanomaterials and Smart Sensors Research Lab (NSSRL), Department of Materials Science and Engineering, HUST, No. 1037, Luoyu Road, Wuhan 430074, PR China

1 H. E. Çamurlu, Ö. Kesmez, E. Burunkaya, N. Kiraz, Z. Yeşil, M. Asiltürk, E. Arpaç, *Chem. Pap.,* 2012, **66**, 461-471.
2 L. Yao, J. H. He, *Prog. Mater. Sci.*, 2014, **61**, 94-143.
3 L. Q. Ye, S. M. Zhang, Q. Wang, L. H. Yan, H. B. Lv, B. Jiang, *RSC Adv.,* 2014, **4**, 35818-35822.
4 X. X. Zhang, M. Y. Zhuang, X. Miao, W. M. Su, M. Y. Lin, L. X. Lin, L. Q. Ye, L. H. Yan, W. B. Yang, B. Jiang, *RSC Adv*., 2014, DOI:10.1039/C4RA05449K.
5 G. S. Vicente, R. Bayon, N. German, A. Morales, *Sol. Energy* 2011, **85**, 676-680.
6 Q. Q. Mao, D. W. Zeng, C. S. Xie, *Mater. Lett.,* 2014, **132**, 214-217.
7 S. Guldin, P. Kohn, M. Stefik, J. Song, G. Divitini, F. Ecarla, C. Ducati, U. Wiesner, U. Steiner, *Nano Lett.,* 2013, **13**, 5329-5335.
8 46 X. X. Zhang, B. B. Xia, H. P. Ye, Y. L. Zhang, B. Xiao, L. H. Yan, H. B. Lv, B. Jiang, *J. Mater. Chem.*, 2012, **22**, 13132-13140.
9 R. Prado, G. Beobide, A. Marcaide, J. Goikoetxea, A. Aranzable, *Sol. Energy Mater. Sol. Cells,* 2010, **94**, 1081-1088.
10 L. Yao, J. H. He, *J. Mater. Chem. A*, 2014, **2**, 6994-7003.
11 Y. K. Lai, Y. X. Tang, J. J. Gong, D. G. Gong, L. F. Chi, C. J. Lin, Z. Chen, *J. Mater. Chem.*, 2012, **22**, 7420-7426.
12 G. Helsch, J. Deubener, *Sol. Energy,* 2012, **86**, 831-836.
13 Z. Y. Liu, X. T. Zhang, T. Murakami, A. Fujishima, *Sol. Energy Mater. Sol. Cells,* 2008, **92**, 1434-1438.
14 E. Burunkaya, Ö. Kesmez, N. Kiraz, H.E. Çamurlu, M. Asiltürk, E. Arpaç, *Mater. Chem. Phys.,* 2010, **120**, 272-276.
15 Z. Geng, J. H. He, L. G. Xu, L. Yao, *J. Mater. Chem. A*, 2013, **1**, 8721-8724.
16 A. Vincent, B. Suresh, E. Brinley, A. Karakoti, S. Deshpande, S. Seal, *J. Phys. Chem. C,* 2007, **111**, 8291-8298.

17 R. Wang, K. Hashimoto, A. Fujishima, M. Chikuni, E. Kojima, A. Kitamura, M. Shimohigoshi, T. Watanabe, *Nature,* 1997, **388**, 431-432.
18 I. P. Parkin, R. G. Palgrave, *J.Mater. Chem*., 2005, **15**, 1689-1695.
19 L. W. Zhang, R. Dillert, D. Bahnemann, M. Vormoor, *Energy Environ. Sci.*, 2012, **5**, 7491-7507.
20 K. S. Liu, M. Y. Cao, A. Fujishima, L. Jiang, *Chem. Rev.,* 2014, DOI: 10.1021/cr4006796.
21 X. Y. Li, J. H. He, *ACS Appl. Mater. Interfaces,* 2013, **5**, 5282-5290.
22 J. G. Cai, J. F. Ye, S. Y. Chen, X. W. Zhao, D. Y. Zhang, S. Chen, Y. R. Ma, S. Jin, L. M. Qi, *Energy Environ. Sci.*, 2012, **5**, 7575-7581.
23 L.J. Gao, J.H. He, *J. Colloid Interface Sci.*, 2013, **400**, 24–30.
24 M. W. Gaultois, A. P. Grosvenor, *J. Mater. Chem*., 2011, **21**, 1829-1836.
25 N. Guo, Y. M. Liang, S. Lan, L. Liu, G. J. Ji, S. C. Gan, H. F. Zou, X. C. Xu, *Appl. Surf. Sci.,* 2014, **305**, 562-574.
26 W. J. Ong, L. L. Tan, S. P. Chai, S. T. Yong, A. R. Mohamed, *Nanoscale*, 2014, **6**, 1946-2008.
27 X. F. Wang, Q. Y. Xiang, B. Liu, L. J. Wang, T. Luo, D. Chen, G. Z. Shen, *Sci. Rep.,* 2013, **3**, 2007.
28 X. Obradors, T. Puig, M. Gibert, A. Queralto, J. Zabaleta, N. Mestres, *Chem. Soc. Rev.*, 2014, **43**, 2200-2225.
29 J. J. Jing, Y. Zhang, W. Y. Li, W. W. Yu, *J. Catal.,* 2014, **316**, 174-181.

